Molecular and Polymer Precursor Routes to Manganese-Doped Zinc Orthosilicate Phosphors

Kai Su,[†,‡] T. Don Tilley,*[,†,‡] and Michael J. Sailor*[,§]

Contribution from the Department of Chemistry, University of California, Berkeley, Berkeley, California 94720-1460, the Chemical Sciences Division, Lawrence Berkeley Laboratory, 1 Cyclotron Road, Berkeley, California 94720, and the Department of Chemistry and Biochemistry, University of California, San Diego, La Jolla, California 92093-0358

Received November 8, 1995[⊗]

Abstract: The zinc alkoxy(siloxy) complex $\{Zn[OSi(O^tBu)_3]_2\}_2$ has been prepared and studied as a molecular precursor to zinc orthosilicate, Zn_2SiO_4. This complex, prepared by reaction of $ZnMe_2$ with $HOSi(O^tBu)_3$, has been characterized by X-ray crystallography as a dimer with two four-coordinate zinc centers. It cleanly looses isobutene, *tert*-butyl alcohol, and $HOSi(O^tBu)_3$ at ca. 100 °C to produce $Zn_2SiO_4 \cdot SiO_2$. Reaction of $ZnMe_2$ with $(HO)_2Si(O^tBu)_2$ affords the hydrocarbon-soluble polymer $[ZnOSi(O^tBu)_2O]_n$, which is proposed to have a structure consisting of four-coordinate Zn atoms linked by bridging $-O(^tBuO)Si(O^tBu)O-$ groups. This polymer undergoes a very clean ceramic conversion over 150−250 °C to give the theoretical yield of carbon-free (by infrared spectroscopy and combustion analyses) $Zn_2SiO_4 \cdot SiO_2$. The pyrolytic elimination products consist of water, *tert*-butyl alcohol, and isobutene. X-ray diffraction studies on the ceramic products show that Zn_2SiO_4 is the only zinc-containing, crystalline product formed. Thus this precursor approach appears to offer an advantage over sol-gel processes, which tend to produce ZnO as a side product. Hydrocarbon solutions of the polymer were used to fabricate high-quality thin films. Via pyrolysis of $[ZnOSi(O^tBu)_2O]_n/[Mn(CH_2SiMe_3)_2]_m$ mixtures, manganese-doped $Zn_2SiO_4 \cdot SiO_2$ materials were synthesized. These materials exhibit two photoluminescence emission bands centered at 535 (major) and 605 nm (minor). The intensity of the green emission at 535 nm, which is responsible for the cathodoluminescence properties of Zn_2SiO_4:Mn phosphors, is highly dependent on the level of manganese doping. Concentration quenching is observed at higher manganese contents. The observed photoluminescence decay lifetime of approximately 5 ms is typical for Zn_2SiO_4:Mn phosphors.

Introduction

Because of its high luminescence efficiency, manganese-doped zinc orthosilicate (willemite, Zn_2SiO_4) has been widely used as a green-emitting phosphor in the display industry,[1] and more recently thin films of Zn_2SiO_4:Mn have been used in the construction of electroluminescent devices.[2] Emission from this material is attributed to a d-level spin-forbidden transition for the Mn^{2+} ions.[1] Traditionally, Zn_2SiO_4:Mn is synthesized in powder form by procedures involving crushing, grinding, ball milling, and high-temperature solid state reactions. However, it is difficult to obtain reliable emission intensities by such methods, probably because of inhomogeneous distributions of metal ions, phase separations, or the accumulation of impurities.[3] For this reason, recent investigations have addressed development of alternative synthetic procedures, and more homogeneous materials with improved emission efficiency have been achieved by sol-gel processes involving the cohydrolysis of soluble silicon, zinc, and manganese compounds, followed by calcination of the resulting gel precursors.[4]

We have been investigating a single-source precursor approach to metal silicate materials. Use of alkoxysiloxy complexes as the molecular precursors allows for molecular-level control over the stoichiometry and homogeneity of the final ceramic.[5] For example, the oxygen-rich precursor complexes $M[OSi(O^tBu)_3]_4$ (M = Zr, Hf) undergo very clean conversions at remarkably low temperatures (100−200 °C) to amorphous, homogeneous MSi_4O_{10} materials, with loss of isobutene and water.[5a] In this paper we describe an application of this approach to the synthesis of zinc silicate materials, starting from both molecular and polymeric zincasiloxane precursors. We were interested in extending our investigations to polymeric precursors, which should offer advantages in processing of the material into a desired shape or form (coatings, films, fibers, monoliths, etc.).[6] Here we show that the poly(zincasiloxane)

[†] University of California, Berkeley.
[‡] Lawrence Berkeley Laboratory.
[§] University of California, San Diego.
[⊗] Abstract published in *Advance ACS Abstracts,* March 1, 1996.

(1) (a) Franz, K. A.; Kehr, W. G.; Siggel, A.; Wieczoreck, J.; Adam, W. In *Ullmann's Encyclopedia of Industrial Chemistry*, 5th ed.; Eivers, B., Hawkins, S., Schulz, G., Eds.; VCH: Weinheim, 1990; Vol. A15, p 519. (b) Leverenz, H. W. *An Introduction to Luminescence of Solids*; John Wiley and Sons, Inc.: New York, 1950. (c) Morell, A.; El Khiati, N. *J. Electrochem. Soc.* **1993**, *140*, 2019. (d) Barthou, C.; Benoit, J.; Benalloul, P. *J. Electrochem. Soc.* **1994**, *141*, 524. (e) Mishra, K. C.; Johnson, K. H.; DeBoer, B. G.; Berkowitz, J. K.; Olsen, J.; Dale, E. A. *J. Luminescence* **1991**, *47*, 197.

(2) (a) Minami, T.; Miyata, T.; Takata, S.; Fukuda, I. *Japanese J. Appl. Phys., Part 2−Letters* **1990**, *30*, L117. (b) Miyata, T.; Minami, T.; Saikai, K.; Takata, S. *J. Luminescence* **1994**, *60&61*, 926.

(3) Chang, I. F.; Brownlow, J. W.; Sun, T. I.; Wilson, J. S. *J. Electrochem. Soc.* **1989**, *136*, 3532.

(4) (a) Morimo, R.; Matae, K. *Mat. Res. Bull.* **1989**, *24*, 175. (b) Morimo, R.; Mochinaga, R.; Nakamura, K. *Mat. Res. Bull.* **1994**, *29*, 751. (c) Khrupunkov, A. N.; Malyavskii, N. I.; Sidorov, V. I. *J. Appl. Chem. USSR* **1989**, *62*, 606. (d) Lin, C.-C.; Shen, P. *J. Non-Cryst. Solids* **1994**, *171*, 281. (e) Watanabe, K. *J. Cryst. Growth* **1991**, *114*, 373.

(5) (a) Terry, K. W.; Tilley, T. D. *Chem. Mater.* **1991**, *3*. 1001. (b) Terry, K. W.; Gantzel, P. K.; Tilley, T. D. *Chem. Mater.* **1992**, *4*, 1290. (c) Terry, K. W., Ph. D. Thesis, University of California at San Diego, 1993. (d) Terry, K. W.; Lugmair, C. G.; Gantzel, P. K.; Tilley, T. D. *Chem. Mater.* **1996**, *8*, 274.

(6) See for example: (a) Jensen, J. A. In *Inorganic and Organometallic Polymers II. Advanced Materials and Intermermediates, ACS Symposium Series 572*; Wisian-Neilson, P., Allcock, H. R., Wynne, K. J., Eds.; American Chemical Society: Washington, D.C., 1994; Chapter 32, p 427. (b) Pouskouleli, G. *Cer. Int.* **1989**, *15*, 213.

0002-7863/96/1518-3459$12.00/0 © 1996 American Chemical Society

$[ZnOSi(O^tBu)_2O]_n$ is an excellent preceramic polymer for the synthesis of Zn_2SiO_4/SiO_2 composites.

Polymetallosiloxanes have been studied for many years as analogs to silicone polymers expected to exhibit high thermal stability and chemical resistance.[7] In fact, some metallosiloxanes have been used as heat stabilizers for siloxane rubbers.[7d] Interest in polymers of this type has recently turned to their pyrolytic decomposition to form metal silicates or metal oxide/silica ceramic composites.[8]

Experimental Section

All synthetic manipulations were performed under an atmosphere of nitrogen or argon using standard Schlenk techniques and/or a Vacuum Atmosphere drybox. Di(*tert*-butoxy)silandiol,[9] tri(*tert*-butoxy)silanol,[10] and $[Mn(CH_2SiMe_3)_2]_n$[11] were prepared according to literature procedures. Di(*tert*-butoxy)silandiol was dried over Drierite in pentane for 0.5 h at room temperature and then crystallized from pentane before use. Dimethylzinc (2.0 M solution in toluene) was purchased from Aldrich and used as received. Trimethylchlorosilane was purchased from Aldrich and distilled before use. Toluene and diethyl ether were freshly distilled from sodium benzophenone.

Infrared spectra were obtained on a Mattson Galaxy Series Fourier transform spectrophotometer. ^1H (400.1 MHz) and ^{13}C (100.6 MHz) NMR spectra were obtained on a Bruker AMX 400 spectrometer equipped with the appropriate decoupling accessories. X-ray powder diffraction (XRD) spectra were recorded on a Sintag XDS 2000 X-ray diffractometer using Cu Kα radiation. The XRD peaks for the oxides and silicates were indexed according to the JCPDS data files (1989). Scanning electron microscopy (SEM) was performed on a Cambridge S360 microscope. Transmission electron micrographs (TEM) were acquired using a Jeol 100 CX microscope. Thermal analyses were performed on a DuPont 951 Thermogravimetric Analyzer attached to either a 910 DSC or 1600 °C DTA cell base. Solution molecular weights were obtained by the Signer method.[12] Elemental analyses were performed at Pascher, Remgen, Germany or at the Microanalytical Laboratory at the University of California, Berkeley. Metal analyses were determined by digesting the samples in HF/HNO_3 and then analyzing the solutions for manganese and zinc content by inductively coupled plasma (ICP) atomic absorption. Steady-state luminescence spectra were obtained using the 365 nm line of a 250 W Hg lamp as excitation source and an Acton 0.275 m monochromator/Princeton Instruments liquid nitrogen-cooled CCD detector and are uncorrected for detector and grating spectral response. Time resolved luminescence data were obtained using a Laser Photonics pulsed N_2 laser (337 nm excitation), 0.125 m monochromator fitted with a Hammamatsu photomultiplier tube, preamplifier, and a Tektronics TDS 520 digital oscilloscope. The instrument-limited time resolution was 100 ns.

$\{Zn[OSi(O^tBu)_3]_2\}_2$. A 2.00 g sample of $(^tBuO)_3SiOH$ (7.58 mmol) in 30 mL of toluene was added dropwise to a 12 mL toluene solution containing 3.79 mmol of dimethylzinc at −40 °C. After the addition, the flask was warmed to room temperature, and the reaction mixture was stirred for 19 h. Vacuum evaporation of the solvent resulted in a viscous oil which slowly crystallized to give 2.00 g (3.38 mmol, 89.2%) of analytically pure $\{Zn[OSi(O^tBu)_3]_2\}_2$ (mp 89 °C dec). Further purification was achieved by recrystallization from hexamethyldisiloxane. Anal. Calcd for $C_{24}H_{54}O_8Si_2Zn$: C, 48.7; H, 9.19; Found: C, 48.2; H, 9.36. Molecular weight in pentane: 570 g mol^{-1}. Calcd for monomer: 592 g mol^{-1}. ^1H NMR (benzene-d_6, 400.1 MHz, 298 K): δ 1.54 ($OCMe_3$). ^1H NMR (toluene-d_8, 300.1 MHz, 223 K): δ 1.55 ($OCMe_3$), 1.59 ($OCMe_3$). $^{13}C\{^1H\}$ NMR (benzene-d_6, 100.6 MHz, 298 K): δ 32.3 ($OCMe_3$), 73.5 ($OCMe_3$). $^{13}C\{^1H\}$ NMR (toluene-d_8, 100.6 MHz, 228 K): δ 31.2 ($OCMe_3$; 2 overlapping peaks), 71.6 ($OCMe_3$), 74.8 ($OCMe_3$). IR (Nujol, NaCl, cm^{-1}): 1460 s, 1448 s, 1382 m, 1362 s, 1243 s, 1190 s, 1065 vs, 1025 s, 913 m, 821 w, 702 m, 649 w, 517 w, 491 w, 425 w.

$\{MeZn[OSi(O^tBu)_3]\}_2$. A 1.00 g sample of $(^tBuO)_3SiOH$ (3.79 mmol) in 10 mL of toluene was added dropwise to a 12 mL toluene solution containing 3.78 mmol of dimethylzinc at −78 °C. After addition, the flask was warmed to room temperature and stirred for 1 h. Vacuum evaporation of the solvent resulted in a viscous oil which crystallized to give 0.89 g (2.59 mmol, 68.3%) of $\{MeZnOSi(O^tBu)_3\}_2$ (mp 50−51 °C). Further purification was achieved by recrystallization from hexamethyldisiloxane. Anal. Calcd for $C_{13}H_{30}O_4SiZn$: C, 45.4; H, 8.79; Found: C, 43.8; H, 8.54. Molecular weight in pentane: 804 g mol^{-1}. Calcd for dimer: 687 g mol^{-1}. ^1H NMR (benzene-d_6, 400.1 MHz): δ 0.06 (ZnMe), 1.36 (O^tBu). $^{13}C\{^1H\}$ NMR (benzene-d_6, 100.6 MHz): δ −11.4 (ZnMe), 31.9 ($OCMe_3$), 73.1 ($OCMe_3$). IR (Nujol, NaCl, cm^{-1}): 1395 m, 1369 m, 1247 m, 1190 s, 1058 vs, 1032 s, 979 m, 920 m, 834 m, 808 w, 710 m, 623 w, 563 w, 524 w, 491 m, 438 w.

$[ZnOSi(O^tBu)_2O]_n$. In a typical reaction, 12.0 mL of a 2.0 M dimethylzinc (24.0 mmol) solution in toluene was added to 30 mL of toluene in a round bottom flask, and then the flask was cooled to −40 °C. A 20 mL toluene solution containing 5.00 g of $(^tBuO)_2Si(OH)_2$ (24.0 mmol) was added dropwise via a cannula, resulting in vigorous methane evolution. After the addition, the reaction mixture was warmed to room temperature and allowed to stir for 2 h. A 6.02 g sample (92.3%) of polymer (**D**) was isolated as a white solid after evaporation of the solvent. Anal. Calcd for $C_8H_{18}O_4SiZn$: C, 35.4; H, 6.68; O, 23.6; Si, 10.3; Zn, 24.1; Found: C, 36.5; H, 6.88; O, 24.9; Si, 10.2; Zn, 21.7. ^1H NMR (benzene-d_6, 400.1 MHz): δ 1.67 (br, O^tBu); $^{13}C\{^1H\}$ NMR (benzene-d_6, 100.6 MHz): δ 32.3 (br, $OCMe_3$), 73.0 ($OCMe_3$). IR (KBr, cm^{-1}): 2985 s, 2949 m, 2895 w, 1488 w, 1397 m, 1379 s, 1253 s, 1208 s, 1073 vs, 1018 vs, 928 s, 820 m, 703 m, 667 w, 531 m, 441 w.

Other polymers were prepared using nonstoichiometric ratios of $ZnMe_2$ and $(^tBuO)_2Si(OH)_2$. For $(^tBuO)_2Si(OH)_2/ZnMe_2$ molar ratios greater than 1, the polymers were prepared by adding a toluene solution of dimethylzinc to a toluene solution of $(^tBuO)_2Si(OH)_2$ which had been cooled to −40 °C, followed by a workup procedure similar to that described above. The reverse addition sequence was used to prepare polymers with $(^tBuO)_2Si(OH)_2/ZnMe_2$ mole ratios less than 1. In each polymerization, ca. 0.50 g of the silanediol was employed. Mole ratios used to prepare polymer samples **A**−**E** are listed in Table 1. The yields for isolated polymers **A**, **B**, **C**, and **E** were 0.50 g (74%), 0.57 g (84%), 0.56 g (85%), and 0.56 g (89%), respectively. The molecular weight properties for these polymers are also summarized in Table 1. The ^1H and ^{13}C NMR spectra for polymers **A**, **B**, **C**, and **E** showed broad resonances for the $-O^tBu$ groups, with chemical shifts consistent with those observed for polymer **D**. The ZnMe end group for polymers **A**, **B**, and **C** appeared as two broad peaks in the ^1H NMR spectra at 0.00 and 0.09 ppm. No end group resonance was identified for **E**. The IR spectra of these polymers are similar, except that **E** exhibited a broad ν(OH) stretching frequency at 3380 cm^{-1}.

Table 1. Molecular Weight Data for Polymers **A**−**E**, as Determined by End-Group Analysis

	$ZnMe_2$/silanediol mole ratio	M_n (calcd)	M_n (obsv)
A	1.156	1802	2170
B	1.067	4110	4200
C	1.025	10905	12300
D	1.000	∞	
E	0.832	1548	25700

Reaction of Polymer E with Me_3SiCl. A 0.10 g sample of polymer **E** was dissolved in 10 mL of toluene, and then 0.05 mL of Me_3SiCl

(7) (a) Voronkov, M. G.; Maletina, E. A.; Roman, V. K. *Heterosiloxanes Volume 1: Derivatives of Non-Biogenic Elements*; Harwood Academic Publishers: Chur, Switzerland, 1988. (b) Hornbaker, E. D.; Conrad, F. *J. Org. Chem.* **1959**, *24*, 1858. (c) Damayeva, A. D. *Polymer Sci. U.S.S.R.*, **1982**, *24*, 996. (d) Andrianov, K. A. *Dokl. Akad. Nauk. SSSR*, **1963**, *281*, 858. (e) Damayeva, A. D. *Polymer Sci. USSR* **1982**, *24*, 996.

(8) (a) Abe, Y.; Gunji, T.; Kimata, Y.; Kuramata, M.; Kasgöz, A.; Misono, T. *J. Non-Cryst. Solids* **1990**, *121*, 21. (b) Gunji, T.; Nagao, Y.; Misono, T.; Abe, Y. *J. Polym. Sci.: Part A: Polymer Chemistry* **1991**, *29*, 941. (c) Gunji, T.; Goto, H.; Kimata, Y.; Nagao, Y.; Misono, T.; Abe, Y. *J. Polym. Sci.: Part A: Polymer Chemistry* **1992**, *30*, 2295. (d) Apblett, A. W.; Warren, A. C.; Barron, A. R. *Chem. Mater.* **1992**, *4*, 167.

(9) Miner, C. S., Jr.; Bryan, L. A.; Holysz, R. P.; Pedlow, G. W. Jr. *Ind. and Engin. Chem.* **1947**, *39*, 1368.

(10) Abe, Y.; Kijima, I. *Bull. Chem. Soc. Jpn.* **1969**, *42*, 1118.

(11) Andersen, R. A.; Carmona-Guzman, E.; Gibson, J. F.; Wilkinson, G. *J. Chem. Soc., Dalton Trans.* **1976**, 2204.

(12) (a) Signer, R. *Leibigs Ann. Chem.* **1930**, *478*, 246. (b) Zoellner, R. W. *J. Chem. Educ.* **1990**, *67*, 714.

Table 2. Analysis of Volatile Decomposition Products from Thermolysis of $[ZnOSi(O^tBu)_2O]_n$ Polymers, as Determined by ^1H NMR Spectroscopy

sample	pyrolysis temp (°C)	pyrolysis time (min)	% conversion of −O^{t}Bu groups	^{t}BuOH/ isobutene molar ratio
polymer **A**[a]	187	13	11	0.2
	300	30	100	0.3
polymer **D**	187	13	30	1
	300	30	100	0.5
polymer **E**	187	6	20	3
	187	13	70	1
	300	30	100	0.6
polymer **F**	300	30	100	0.5
$[MeZnOSi(O^tBu)_3]_2$[a]	300	30	*b*	0.1
$\{Zn[OSi(O^tBu)_3]_2\}_2$	300	30	*b*	0.2

[a] For this sample, methane (not quantified) was also observed as a volatile decomposition product. [b] For this sample, $(^tBuO)_3SiOH$ (not quantified) was also observed as a volatile decomposition product.

(0.39 mmol) was added via a syringe. After being stirred at room temperature for 2 h, the solvent was evaporated to give 0.08 g (80%) of the white polymer (**F**). ^1H NMR (benzene-d_6, 400.1 MHz): δ 1.67 (br, O^{t}Bu); 0.45 ($SiMe_3$). IR (Nujol, NaCl, cm^{-1}): 1380 s, 1309 m, 1251 w, 1285 w, 1153 m, 1069 m, 477 m, 438 w, 737 s, 520 w.

Thermolysis of $\{Zn[OSi(O^tBu)_3]_2\}_2$. A 1.02 g (1.72 mmol) sample of $\{Zn[OSi(O^tBu)_3]_2\}_2$ in a zirconia crucible was heated in a Lindberg tube furnace under a flow of argon. The sample was heated at a rate of 10 °C/min to 1100 °C, and this temperature was maintained for 1 h before the sample was allowed to cool to room temperature. A light grey solid (0.19 g, 19%) was obtained. Anal. Found: Zn, 30.18.

Thermolysis of $[ZnOSi(O^tBu)_2O]_n$. A sample of the polymer was weighed into a zirconia crucible in the glovebox and quickly transferred into a Lindberg tube furnace under a counter flow of argon. The furnace was then purged with argon for an additional 10 min before heating was initiated. Under a continuous flow of argon, 0.52, 0.71, 0.50, and 0.31 g samples were heated to 500, 800, 1100, and 1350 °C, respectively, at 10 °C/min and held at each temperature for 1 h before cooling to room temperature. These pyrolyses yielded 0.27 g (51.9%), 0.35 g (49.3%), 0.24 g (48.0%), and 0.14 g (45.2%) of colorless samples, respectively. For thermolyses to temperatures >500 °C, all subsequent manipulations of the ceramics were carried out in air. Anal. Calcd for $Zn_2SiO_4{\cdot}SiO_2$: Zn, 46.2; Si, 19.9; O, 33.9. Found for sample heated to 1100 °C: C, <0.2; H, <0.1; Si, 22.0; Zn, 41.6; O, 36.2. Found for sample heated to 500 °C: Zn, 41.4; C, 0.20; H, 0.48.

Samples for NMR studies of the ceramic conversion reactions were prepared by placing polymer samples (20−100 mg) in a Schlenk tube and then heating the sample with an oil bath to 190, 210, or 300 °C under a static vacuum. The volatile decomposition products were vacuum-transferred into an NMR tube containing benzene-d_6 and a weighed amount of ferrocene standard at −196 °C. The volatile products were quantified via integrations against the ferrocene standard (Table 2).

Preparation of $Zn_2SiO_4{\cdot}SiO_2$ Films. Dry glass slides that were precleaned by rinsing with acetone and hexanes were dipped into a 2.3% (w/w) solution of polymer **D** in dimethoxyethane (DME). Some of the polymer solution was then removed from the slides by absorption onto a Kimwipe tissue that was brought into contact with the side of the slide. The polymer-coated slides were then transferred quickly into a tube furnace. The samples were heated at 2 °C/min to 500 °C and then held at this temperature for 1 h under a flow of argon before cooling to room temperature.

Mn-Doped $Zn_2SiO_4{\cdot}SiO_2$. $[ZnOSi(O^tBu)_2O]_n/[Mn(CH_2SiMe_3)_2]_m$ polymer mixtures were prepared by dissolving the polymers in diethyl ether and then evaporating the solvent under vacuum. The solid mixtures were then weighed into a zirconia crucible in a glovebox and quickly transferred into a Lindberg tube furnace. Under a purge of argon, the samples were heated at a rate of 10 °C/min to 1100° and then held at this temperature for 1 h. After cooling to room temperature, the ceramic samples were reheated to 1100 °C (20 °C/min) under a flow of wet argon (argon bubbled through a water trap; this leads to consistently white samples and brighter luminescence). After being held at 1100 °C for 1 h, the samples were cooled to room temperature. The samples were then analyzed to determine their manganese and zinc contents.

Table 3. Crystallographic Data for $\{Zn[OSi(O^tBu)_3]_2\}_2$

formula	$Zn_2Si_4O_{16}C_{48}H_{108}$
space group	$P\bar{1}$
Z	4
cell constants	
a(Å)	12.0063 (20)
b(Å)	14.6059 (20)
c(Å)	20.278 (3)
α(°)	88.650 (11)
β(°)	88.006(13)
γ(°)	71.526(12)
V (Å^3)	3364.5 (12)
μ (cm^{-1})	8.5
D_{calc} (g/cm^3)	1.17
F(000)	496
radiation	Mo K$_\alpha$ (λ = 0.71073 Å)
θ range, deg	3.0−45.0
scan mode	ω−2θ
no. reflcns measd	8768
no. unique reflcns	8768
R_f	5.23%
R_{wf}	6.22%
GOF	1.77

Structure Determination for $\{Zn[OSi(O^tBu)_3]_2\}_2$. Clear, colorless prisms of the compound were obtained by slow crystallization from hexamethyldisiloxane at −40 °C. Fragments cleaved from some of these crystals were mounted on a glass fiber using Paratone N hydrocarbon oil. X-ray intensity data were collected at −110 °C on an Enraf-Nonius CAD-4 diffractometer equipped with a nitrogen flow low-temperature apparatus which was previously calibrated by a thermocouple placed at the sample position. Crystallographic data are listed in Table 3. The unique raw intensity data were converted to structure factor amplitudes and their esds by correction for scan speed, background, and Lorentz and polarization effects. No correction for crystal decomposition was necessary. Inspection of the azimuthal scan data showed a variation I_{min}/I_{max} = 0.96 for the average curve. No correction for absorption was applied.

The structure was solved by Patterson methods and refined via standard least-squares and Fourier techniques. Several of the *tert*-butoxy groups were disordered. The disordered atoms were modeled with isotropic half-occupancy atoms. In a difference Fourier map calculated following the refinement of all ordered non-hydrogen atoms with anisotropic thermal parameters, peaks were found corresponding to the positions of many of the hydrogen atoms. Hydrogen atoms attached to ordered carbon atoms were assigned idealized locations and values of B_{iso} approximately 1.3 times the B_{eqv} of the atoms to which they were attached. They were included in structure factor calculations but not refined. Hydrogen atom positions were not calculated for disordered carbon atoms. Inspection of the residuals ordered in ranges of sin θ/λ, $|F_o|$, and parity and value of the individual indexes showed no unusual features or trends. The largest peak in the final difference Fourier map had an electron density of 0.69 e$^-$/Å^3, near the disordered −O^{t}Bu carbon atoms.

Results and Discussion

Synthesis of Molecular Precursors. Our previous studies on molecular precursor routes to metal oxide materials have shown that tri(*tert*-butoxy)siloxy complexes such as $Zr[OSi(O^tBu)_3]_4$ and $\{AlMe_2[OSi(O^tBu)_3]\}_2$ cleanly eliminate isobutene and water at low temperatures to give ZrO_2/SiO_2 and Al_2O_3/SiO_2 ceramics in very high yield.[5] These results suggested that similar zinc complexes might be useful as processible, high-yield precursors to zinc orthosilicate, Zn_2SiO_4. Furthermore, it was thought that such a precursor route to Zn_2SiO_4 would be amenable to homogeneous doping with metal ions to give phosphorescent materials.

Table 4. Selected Bond Distances (Å) and Angles (deg) for $\{Zn[OSi(O^tBu)_3]_2\}_2$

			Distances		
Zn1−O1	1.870 (4)	Zn1−O4	2.258 (4)	Zn1−O9	1.940 (4)
Zn1−O13	1.940 (4)	Zn2−O13	1.956 (4)	Zn2−O9	2.141 (4)
Zn2−O10	2.124 (4)	Zn2−O5	1.798 (5)	Si3−O9	1.579 (5)
Si3−O10	1.663 (5)	Si3−O11	1.600 (5)	Si1−O1	1.594 (5)
Si1−O4	1.662 (5)	Si4−O13	1.613 (5)	Si2−O5	1.556 (5)
			Angles		
O1−Zn1−O4	72.7 (2)	O1−Zn1−O9	132.4 (2)	Si1−O1−Zn1	102.6 (2)
Si1−O4−Zn1	86.0 (2)	O1−Si1−O4	98.4 (2)	Zn1−O9−Zn2	91.1 (2)
O9−Zn2−O13	81.8 (2)	Zn2−O13−Zn1	97.0 (2)	O13−Zn1−O9	87.7 (2)
Si3−O9−Zn2	96.8 (2)	Si3−O10−Zn2	95.32 (2)	Si4−O13−Zn2	121.8 (3)
Zn1−O9−Si3	128.1 (3)	O13−Zn2−O10	117.0 (2)	Zn2−O5−Si2	158.2 (4)

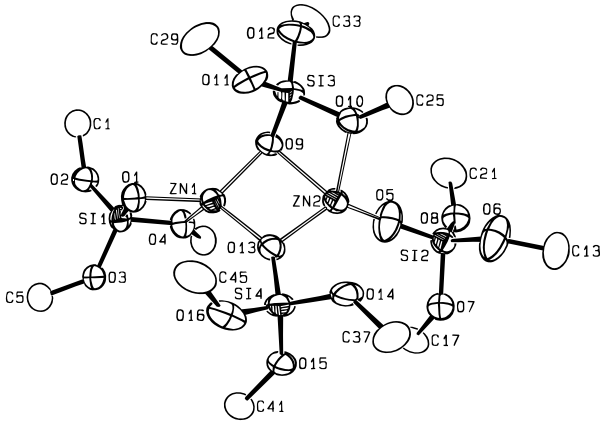

Figure 1. ORTEP drawing of $\{Zn[OSi(O^tBu)_3]_2\}_2$. The methyl carbon atoms are omitted for clarity.

The zinc siloxide $\{Zn[OSi(O^tBu)_3]_2\}_2$ was obtained by reaction of 2 equiv of $HOSi(O^tBu)_3$ with dimethylzinc in toluene solution at −40 °C (eq 1). The compound is obtained in nearly quantitative yield (by NMR spectroscopy) as a colorless, air- and moisture-sensitive solid upon removing solvent from the reaction mixture. Recrystallization is achieved by cooling a saturated hexamethyldisiloxane solution to low temperature.

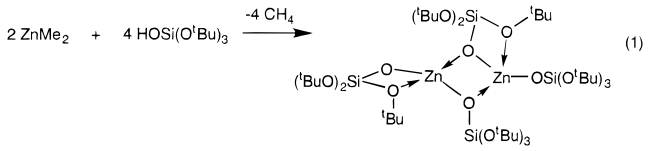

(1)

The molecular structure of this zinc siloxide complex is shown in the ORTEP drawing of Figure 1, and selected bond distances and angles are given in Table 4. The compound exists as asymmetric dimers with four $-OSi(O^tBu)_3$ ligands which each exhibit distinct coordination modes ($\eta^1;\eta^2;\mu\text{-}\eta^1,\eta^1;\mu\text{-}\eta^1,\eta^2$). Rotational disorder in four of the *tert*-butoxy groups and relatively close contacts between the disordered methyl groups (ca. 3.36 Å) indicate some degree of steric crowding in the molecule. The coordination geometries for the zinc centers may be described as tetrahedrons which are severely distorted (toward trigonal pyramids) by the small angles imposed by chelation of the $OSi(O^tBu)_3$ ligands, the four-membered ring imposed by dimer formation, and the inequivalent Zn−O distances. The Zn atoms are close to planes defined by three of their ligated oxygen atoms (Zn1 lies 0.224 Å above the O1−O9−O13 plane, and Zn2 lies 0.099 Å above the O5−O10−O13 plane). The zinc−oxygen distances are highly dependent upon the types of oxygen atoms involved in the bonding: $Zn-O_{terminal}$ (1.798(5) and 1.870(4) Å), $Zn-O_{bridging}$ (1.940(4), 1.940(4), 1.956(4), and 2.141(4) Å), and $Zn-O_{etheric}$ (2.124(4) and 2.258(4) Å). The remaining bond distances and angles are normal and similar to those observed in other siloxane complexes.[5,13] The Zn_2O_2 four-membered ring is essentially flat and forms angles of 83.79° and 125.9° with the Si1−O1−Zn1−O4 and O9−Si3−O10−Zn2 planes, respectively.

A molecular weight determination for the compound (570 g mol^{-1} in pentane; calcd for monomer: 592 g mol^{-1}) supports a monomeric structure in solution. Solution NMR studies on this complex revealed temperature-dependent behavior. Thus, the room temperature proton NMR spectrum of the complex shows only a singlet at 1.56 ppm corresponding to the *tert*-butoxy protons. However, when the complex was cooled to −40 °C in toluene-d_8, this resonance split into two peaks with an intensity ratio of 1:1, indicating the presence of two sets of *tert*-butoxy groups. A variable-temperature study provided an activation energy of $\Delta G^{\ddagger} = 13$ kcal mol^{-1} ($T_c = 241$ K) for this process. Similarly, the ^{13}C NMR spectrum at −40 °C exhibited resonances arising from two sets of *tert*-butoxy carbon atoms. No further splitting was observed in ^1H and ^{13}C NMR spectra when the sample was cooled to −80 °C. Based on these observations, we presume that a monomer−dimer equilibrium exists in solution. Furthermore, it appears that bridging and terminal siloxide ligands for the dimer do not exchange on the NMR time scale at −80 °C, but each pair of terminal and bridging ligands interconvert rapidly above −80 °C via dissociation/association of the O → Zn dative bonds.

The reaction of dimethylzinc with 1 equiv of tris(*tert*-butoxy)-silanol in toluene gave $[MeZnOSi(O^tBu)_3]_2$, which was isolated in high yield as a white solid upon vacuum evaporation of the solvent (eq 2). With slow addition of the silanol to $ZnMe_2$ at

$$2ZnMe_2 + 2HOSi(O^tBu)_3 \xrightarrow{-2CH_4} \{MeZn[\mu\text{-}OSi(O^tBu)_3]\}_2 \quad (2)$$

low temperature (−40 °C), the reaction is quantitative. A molecular weight determination for $[MeZnOSi(O^tBu)_3]_2$ (804 g mol^{-1} in pentane) is most consistent with formulation of the complex as a dimer (Calcd: 687 g mol^{-1}). The proton NMR spectrum of the compound shows two resonances in a 1:9 ratio at 0.06 and 1.36 ppm, arising from the Zn−Me and $-O^tBu$ protons, respectively. The ^{13}C NMR spectrum shows resonances at 31.9 and 73.1 ppm corresponding to *tert*-butoxy carbon atoms and a peak at −11.4 ppm resulting from the ZnMe group. Previously reported $[RZnOSiR'_3]_n$ (R = alkyl or aryl) complexes were found to exist either in dimeric or tetrameric form, depending on the nature of the substituents.[7a]

Solid-State Thermolysis of $\{Zn[OSi(O^tBu)_3]_2\}_2$. The molecular precursor $\{Zn[OSi(O^tBu)_3]_2\}_2$ readily undergoes ther-

(13) (a) McMullen, A. K.; Tilley, T. D.; Rheingold, A. L.; Geib, S. J. *Inorg. Chem.* **1989**, *28*, 3772. (b) Terry, K. W.; Gantzel, P. K.; Tilley, T. D. *Inorg. Chem.* **1993**, *32*, 5402.

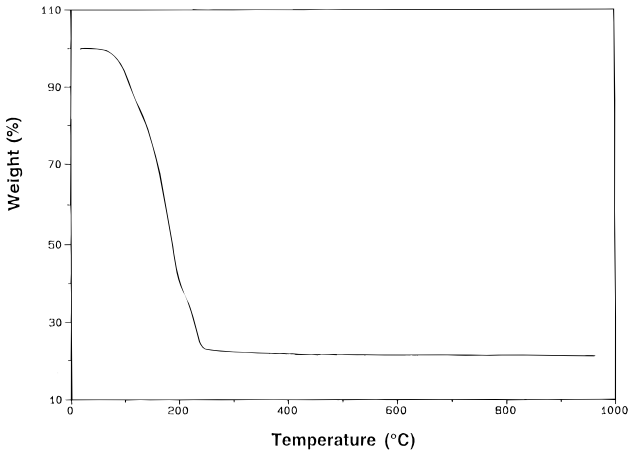

Figure 2. Thermal gravimetric analysis (TGA) of $\{Zn[OSi(O^tBu)_3]_2\}_2$.

molysis to zinc orthosilicate-silica composite materials. The thermal gravimetric analysis (TGA) of $\{Zn[OSi(O^tBu)_3]_2\}_2$, shown in Figure 2, reveals a facile weight loss which begins at ca. 100 °C and is complete by 250 °C. The observed ceramic yield (22%) is significantly lower than the theoretical value (34%) for conversion to a 1:3 Zn_2SiO_4:SiO_2 composite. The differential scanning calorimetry (DSC) analysis revealed an endothermic event in the temperature region 57−69 °C prior to thermal decomposition, which could correspond to melting or a solid-state phase transformation for the complex, although sharp melting at 89 °C (with decomposition) was observed with a standard melting point apparatus. Differential thermal analysis (DTA) revealed endothermic events in the 100−280 °C temperature range corresponding to thermal decomposition of the complex, and crystallization of Zn_2SiO_4 results in an exothermic peak at 803 °C (vide infra).

The stoichiometry for thermal decomposition of $[Zn[OSi(O^tBu)_3]_2\}_2$ at 300 °C was established by trapping the volatile decomposition products under vacuum. The volatile products that were condensed in an NMR tube containing benzene-d_6 and a measured amount of ferrocene standard at −196 °C were shown by ^{1}H NMR analysis to be *tert*-butyl alcohol and isobutene in a 1:5 ratio. Some colorless crystals that sublimed during the pyrolysis but were not transferred to the NMR tube were identified as $HOSi(O^tBu)_3$ (by NMR spectroscopy). The loss of silanol during the pyrolysis is in agreement with the observed low ceramic yield and suggests the reaction stoichiometry of eq 3. For this process, the calculated ceramic yield is 24%, in good agreement with the observed yield of 22%. An

$$\{Zn[OSi(O^tBu)_3]_2\}_2 \xrightarrow{\Delta} Zn_2SiO_4{\cdot}SiO_2 + 2HOSi(O^tBu)_3 + 5CH_2{=}CMe_2 + HO^tBu + H_2O \quad (3)$$

X-ray powder diffraction (XRD) analysis of this material (obtained by bulk pyrolysis at 1100 °C for 1 h; Figure 3) revealed the presence of willemite, but cristobalite could not be definitively identified. This material was also examined by transmission electron microscopy (TEM) (Figure 4a), which shows the presence of irregularly-shaped particles that are approximately 50−100 nm in diameter.

Synthesis of the Polymeric Precursor $[ZnOSi(O^tBu)_2O]_n$. In attempts to develop a precursor which might exhibit better processibility and a higher ceramic yield, we pursued the synthesis of a zinc siloxane polymer which would also readily transform to zinc orthosilicate. Our approach was based on the reaction of dimethylzinc with the known silanediol $(HO)_2Si(O^tBu)_2$.[9] The synthesis of polyzincadiphenylsiloxane, $[ZnOSiPh_2O]_n$, isolated as an insoluble material contaminated with zinc oxide, from reaction of $ZnEt_2$ with $Ph_2Si(OH)_2$, was reported previously by Hornbraker and Conrad.[7b] Soluble oligo- and polyzincaorganosiloxanes have also been obtained from reaction of alkyltrichlorosilane or alkyltriethoxysilane with zinc acetate and from reaction of organosiloxanediolates with zinc halides.[14] Related polymers $[-Ti(acac)_2-OSi(OR)_2O-]_n$ have also been obtained from the diols $(HO)_2Si(O^tBu)_2$ and $(HO)_2Si[OSi(O^tBu)_3]_2$.[8a,15]

The compound $(HO)_2Si(O^tBu)_2$ may be obtained by hydrolysis of $(H_2N)_2Si(O^tBu)_2$ with ice−water, as described in the

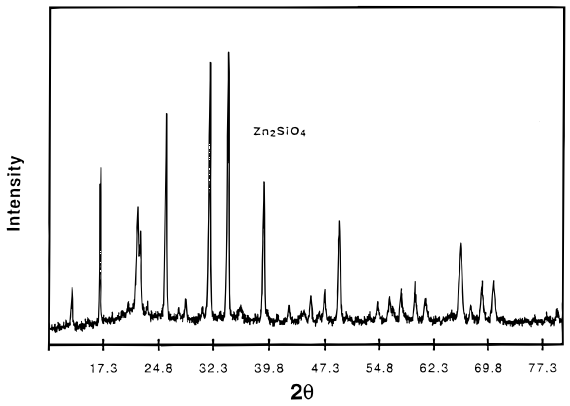

Figure 3. X-ray powder diffraction (XRD) pattern for the ceramic material derived from $\{Zn[OSi(O^tBu)_3]_2\}_2$ (heated at 1100 °C for 1 h), showing the presence of Zn_2SiO_4. The peak near $2\Theta = 17°$ is due to the sample holder.

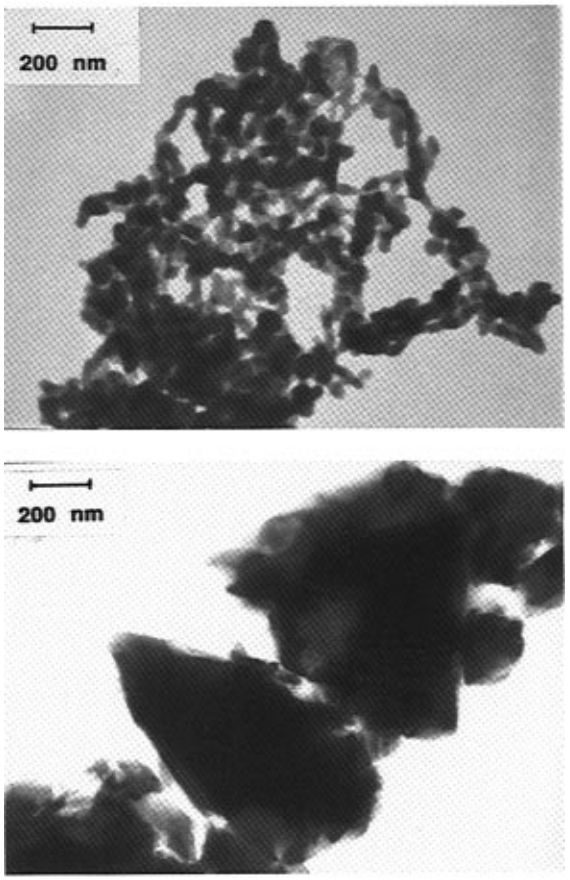

Figure 4. (a, top) Transmission electron micrograph (TEM) of ceramic particles derived from pyrolysis of $\{Zn[OSi(O^tBu)_3]_2\}_2$ (at 1100 °C for 1 h). (b, bottom) Transmission electron micrograph (TEM) of $Zn_2SiO_4{\cdot}SiO_2$ derived from heating polymer **D** at 1100 °C for 1 h.

literature.[9] The product separates as a crystalline solid which is quite sensitive to condensation polymerization in organic solvents. Brief drying of a pentane solution of the silanediol over Drierite (0.5 h), and recrystallization twice from pentane, gave pure product which was then stable at room temperature in the solid state for months.

The 1:1 reaction of $ZnMe_2$ and $(HO)_2Si(O^tBu)_2$ proceeds smoothly at −40 °C in toluene with evolution of methane to give a polyzincasiloxane polymer which was isolated as a slightly moisture-sensitive white solid after evaporation of the solvent (eq 4). The polymer is readily soluble in common organic solvents such as hydrocarbons or ethers but does not melt before onset of decomposition at ca. 90 °C.

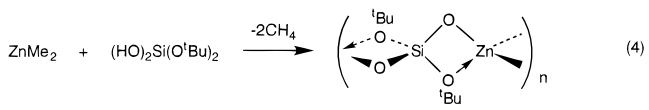

(4)

Total elemental analysis of the polymer is approximately consistent with the formula $[ZnOSi(O^tBu)_2O]_n$. The ^1H NMR spectrum shows only one broad resonance centered at 1.67 ppm, which is attributed to the *tert*-butoxy side groups. No end group resonances were detected in this spectrum. Also, the ^{13}C NMR spectrum exhibits two broad peaks for the ^{t}BuO groups, centered at 32.3 and 73.0 ppm. We propose a structure for the polymer involving bridging *tert*-butoxy groups, as depicted in eq 4, with the zinc centers in their preferred four-coordinate environment. The proposed bonding of the zinc atoms to chelating siloxy/*tert*-butoxy functions is similar to one of the metal−ligand interactions observed in the crystal structure of $\{Zn[OSi(O^tBu)_3]_2\}_2$ (which forms the Si1−O1−Zn1−O4 four-membered ring). Zinc compounds containing β-hydroxyl siloxy groups, $(RSi(OH)_2O)_2Zn$ (R = C_2H_5 or C_6H_5), have been proposed to have related monomeric chelate structures involving coordination of the hydroxyl oxygen to the zinc centers.[16]

Molecular weight determinations by gel permeation chromatography were unsuccessful due to apparent adherence or decomposition of the polymer on the columns. An attempted solution molecular weight determination by vapor phase osmometry, using polystyrene standards, was successful only in indicating that the molecular weight was greater than ca. 40 000 g mol^{-1}. For this reason, we attempted to investigate the molecular weight properties for lighter polymers containing observable end groups.

A series of polymers were prepared using nonstoichiometric ratios of $ZnMe_2$ and $(HO)_2Si(O^tBu)_2$, as described in the Experimental Section and Table 1. The ^1H NMR spectra for polymers **A**, **B**, and **C** exhibit similar *tert*-butoxy resonances in addition to broad peaks at 0.0 and 0.1 ppm which are assigned to ZnMe end groups. These resonances increase in intensity with increasing $ZnMe_2$/silanol ratios. The chemical shifts for the latter resonances are similar to those observed for the ZnMe protons in $[MeZn(OSi(O^tBu)_3]_2$. The presence of two Zn−Me resonances for the polymers apparently reflects different coordination environments for zinc atoms in the end groups. The polymer prepared with the silanediol in excess (**E**) did not exhibit an identifiable hydroxy end group in its ^1H NMR spectrum, and only one broad resonance for overlapping internal *tert*-butoxy and $-Si(O^tBu)_2OH$ end groups was observed, at 1.6 ppm. However, the IR spectrum for polymer **E** contained a broad absorption at 3300 cm^{-1} due to the OH group in $-Si(O^tBu)_2OH$.

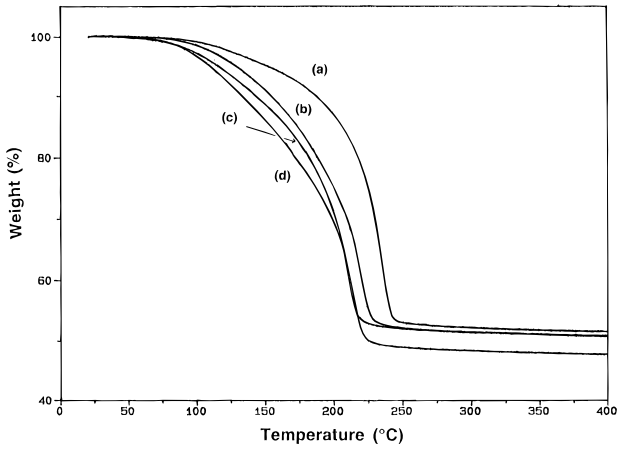

Figure 5. Thermal gravimetric analyses (TGA) for $[ZnOSi(O^tBu)_2O]_n$ polymers: (a) polymer **A**, (b) polymer **D**, (c) polymer **E**, (d) polymer **F**.

Molecular weight data for polymers **A**−**C** and **E** was obtained by end-group analysis from ^1H NMR spectroscopy. For polymers terminated by Zn−Me groups, the molecular weights were determined by integration of the Zn−Me and $-OCMe_3$ resonances. As shown in Table 1, the polymer prepared from a 1.156 $ZnMe_2$/silanediol ratio has a number average molecular weight of 2170 g mol^{-1}, which is close to the expected value of 1802 g mol^{-1} based on quantitative condensation of dimethylzinc with silanediol. When the monomer molar ratio was decreased to 1.025 (**C**), a significant increase in the molecular weight (to M_n(obsvd): 12 300 g mol^{-1}; M_n(calcd): 10 905 g mol^{-1}) was observed. For polymer **E**, the $-Si(O^tBu)_2OH$ end groups were not detected by NMR spectroscopy. However reaction of this polymer with Me_3SiCl appeared to cleanly convert the terminal −OH groups to $-OSiMe_3$ groups (to give polymer **F**), which were clearly observed in the ^1H NMR spectrum. The average molecular weight for **E**, estimated by comparing the relative intensities of the $-OSiMe_3$ and $-O^tBu$ groups, was calculated to be 25 700. This number is far greater than the expected value of 1550, implying incomplete conversion of −OH to $-OSiMe_3$ groups or that condensation of the hydroxy end groups might have occurred to increase the molecular weight. Determination of the molecular weight for polymer **D** by this method was not possible, due to the absence of observable end groups.

Ceramic Conversion of $[ZnOSi(O^tBu)_2O]_n$ to $Zn_2SiO_4 \cdot SiO_2$. The ceramic conversion reaction of $[ZnOSi(O^tBu)_2O]_n$ polymer to zinc orthosilicate was investigated prior to attempts to prepare manganese-doped materials. TGA analysis of the ceramic conversion reaction for **D** (Figure 5, curve b) shows an onset of weight loss at ca. 60 °C, and completion of the transformation by 230 °C. A 52.1% ceramic yield was observed for polymer **D**, which is in good agreement with the theoretical ceramic yield corresponding to formation of $Zn_2SiO_4 \cdot SiO_2$ (52.2%). The DTA curve for **D**, shown in Figure 6, exhibits an endotherm at 234 °C resulting from polymer decomposition, followed by an exotherm corresponding to crystallization of Zn_2SiO_4. In agreement with the thermal analysis results, infrared spectra of the ceramic sample obtained by heating polymer **D** at 300 °C for 30 min contain no C−H stretching modes, indicating

(14) (a) Kirichenko, E. A.; Damaeva, A. D.; Markov, B. A.; Ivanova, S. M.; Ermakov, A. I. *Vysokomol. Soedin., Ser. A* **1975**, *17*, 1482. (b) Damaeva, A. D.; Mashutina, G. G.; Kirichenko, E. A. *Vysokomol. Soedin., Ser. A* **1982**, *24*, 11684. (c) Damaeva, A. D.; Popov, V. M.; Kirichenko, E. A.; Khananashvili, A. M. *Soobshch. Akad. Nauk. GSSR* **1981**, *104*, 609. (d) Damaeva, A. D.; Kirichenko, E. A. *Khimiya i Khimich. Tekhnol.* **1972**, *15*, 954.

(15) (a) Abe, Y.; Kijima, I. *Bull. Chem. Soc. Jpn.* **1970**, *43*, 466. (b) Kijima, I.; Yamamoto, T.; Abe, Y. *Bull. Chem. Soc. Jpn.* **1971**, *44*, 3193.

(16) Zhdanov, A. A.; Andrianow, K. A. *Izv. Akad. Nauk. SSSR. Ser.* **1976**, 395.

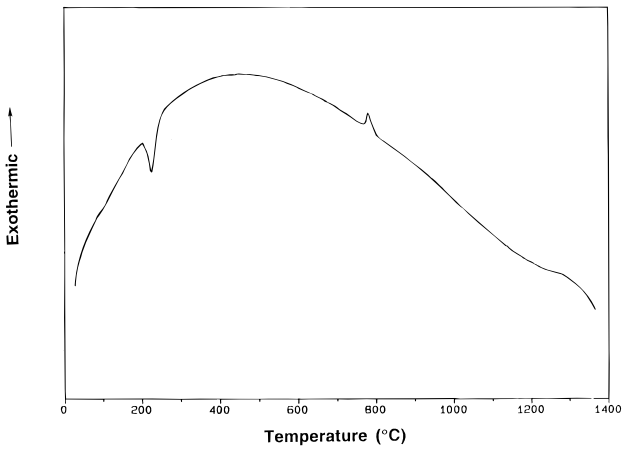

Figure 6. Differential thermal analysis (DTA) for polymer **D**.

complete conversion to the ceramic material at this temperature. Broad absorptions at 900−950 cm^{-1} and 550 cm^{-1} are consistent with the presence of Si−O−Zn linkages.[17]

Bulk pyrolysis of polymer **D** at 500, 850, 1100, and 1350 °C under argon gave silicate ceramics in 51.9%, 49.3%, 48.0%, and 45.2% ceramic yields, respectively. The material heated to 1100 °C exhibited an elemental composition consistent with the formation of a $(Zn_2SiO_4)_{0.37}(SiO_2)_{0.41}$ composite. The carbon and hydrogen contents for the material heated to 500 °C are 0.20% and 0.48%, respectively (by combustion analysis). Significantly less carbon (<0.2%) and hydrogen (<0.1%) were found in the ceramic material heated at 1100 °C for 1 h.

Previous studies on the thermal decomposition of polymetallosiloxanes and related polymetalloxanes have described complex chemistry which is highly dependent on the nature of the substituents on the polymer backbone. However, these polymers have typically been characterized as heat-resistant and thermally stable.[7a,18] Damayeva examined the thermal properties of a number of oligo-metallophenylsiloxanes, which decomposed at temperatures above 800 °C with elimination of small organic molecules including benzene. The residues remaining after decomposition were not identified.[7c] In other systems, decomposition occurs at lower temperature to give metal oxides and siloxanes. For example, polyzincadiphenylsiloxane polymer $[ZnOSiPh_2O]_n$ undergoes redistribution upon heating to give hexaphenyltrisiloxane-1,5-diol and zinc oxide.[7b] Thus, it appears that the polyzincasiloxane polymer described here is unique among metallosiloxane polymers in that it undergoes clean elimination of organic fragments to form a metal silicate, rather than an oxide, as the final product.

Analysis of the volatile materials from pyrolysis of $[ZnOSi(O^tBu)_2O]_n$ by ^1H NMR spectroscopy revealed the presence of water, ^{t}BuOH, and isobutene, as summarized in eq 5 and Table

$$[ZnOSi(O^tBu)_2O]_n \rightarrow \frac{n}{2}Zn_2SiO_4 + \frac{n}{2}SiO_2 + xH_2O + (n-x)HOCMe_3 + (n+x)CH_2{=}CMe_2 \quad (5)$$

2. Thermolysis of polymer **D** at 187 °C for 13 min gave a 1:1 ratio of *tert*-butyl alcohol and isobutene. When this polymer was pyrolyzed at 300 °C for 30 min, the volatile products were identified as isobutene, *tert*-butyl alcohol, and water, with a *tert*-butyl alcohol/isobutene ratio of 1:2. The pyrolysis at 300 °C gave the theoretical ceramic yield and a material containing no residual hydrocarbon (by IR spectroscopy); thus the observed volatile species should fairly accurately reflect the final distribution of decomposition products.

A simple mechanism which can explain the observed elimination products is given in Scheme 1. The initial step in this process involves heterolytic cleavage of the oxygen−carbon bond to give a carbocation and a basic oxygen center.[19] Subsequent proton transfer from the *tert*-butyl cation to oxygen results in formation of isobutene and a silanol group in the polymer backbone. Condensation to a larger network may then occur via reactions of silanol and *tert*-butoxy groups (path a) or silanol−silanol condensations (path b). This mechanism is highly speculative, and alternative schemes involving a more concerted "*β*-hydrogen elimination" of the *tert*-butoxy groups,[20] autocatalytic decomposition,[21] Bronsted acid-catalyzed eliminations,[5c] or homolytic cleavages[22] should also be considered.

The observed differences in the distribution of volatile decomposition products as a function of conversion may be rationalized in terms of the proposed mechanism. Early in the reaction, isobutene elimination presumably leads to a low concentration of silanol functionalities (not detectable by IR) in the presence of a relatively high concentration of O^{t}Bu groups. Thus, path (a) predominates and a higher ^{t}BuOH/$CH_2{=}CMe_2$ ratio is observed. As the reaction proceeds, the number of −O-^{t}Bu groups is reduced, and the network becomes less mobile, resulting in condensations predominantly via silanol groups and a lower ^{t}BuOH/$CH_2{=}CMe_2$ ratio. The increased amount of isobutene at higher conversion may also be explained by water elimination of *tert*-butyl alcohol under pyrolytic conditions;[20a,23] however, it should be noted that the pyrolyses were carried out in vacuo and the volatile materials were rapidly trapped at −196 °C.

As shown by the data in Table 2, the observed distribution of elimination products at low conversions is sensitive to the nature of the polymer end groups. The presence of SiOH end groups is associated with initial formation of more ^{t}BuOH (vs isobutene), whereas proton-scavenging Zn−Me end groups (polymer **A**) result in the production of more isobutene. The latter pyrolysis produced significant quantities of methane early in the reaction. Related effects are also seen by comparing the TGA curves for polymer samples **A**, **D**, **E**, and **F**, which show that the presence of silanol end groups results in a somewhat more facile decomposition (Figure 5). Thus, it would seem that these pyrolytic elimination reactions may be catalytic in nature. Our previous studies on the thermal decomposition of $Zr[OSi(O^tBu)_3]_4$ in solution suggest operation of a H^+-catalyzed mechanism for production of isobutene, water, and *trace* amounts of *tert*-butyl alcohol.[5c,24] Bradley[21a,b] and Chisholm[21c] have observed autocatalytic decompositions for metal alkoxide species in the presence of small quantities of water.

X-ray powder diffraction studies of the ceramic products revealed the evolution of crystalline phases as the processing

(17) (a) Hurt, J. C.; Phillips, C. J. *J. Am. Ceram. Soc.* **1970**, *53*, 296. (b) Lin, C.; Shen, P. *J. Non-Cryst. Solids* **1994**, *171*, 281.

(18) Kirichenko, E. A.; Damaeva, A. D.; Markov, B. A.; Ivanova, S. M.; Ermakov, A. I. *Vysokomol. Soedin., Ser. A* **1975**, *17*, 1482.

(19) (a) Knözinger, H. *Angew. Chem., Int. Ed. Engl.* **1968**, *7*, 791. (b) Noller, H.; Andréu, P.; Hunger, M. *Angew. Chem. Int., Ed. Engl.* **1971**, *10*, 172.

(20) (a) Lundeen, A. J.; Van Hoozer, R. *J. Org. Chem.* **1967**, *32*, 3386. (b) Jeffries, P. M.; Dubois, L. H.; Girolami, G. S. *Chem. Mater.* **1992**, *4*, 1169. (c) Budzichowski, T. A.; Chisholm, M. H.; Strieb, W. E. *J. Am. Chem. Soc.* **1994**, *116*, 389.

(21) (a) Bradley, D. C.; Faktor, M. M. *J. Chem. Soc., Faraday Trans.* **1959**, *55*, 2117. (b) Bradley, D. C. *Chem. Rev.* **1989**, *89*, 1317. (c) Baxter, D. V.; Chisholm, M. H.; DiStasi, V. F.; Klang, J. A. *Chem. Mater.* **1991**, *3*, 221.

(22) (a) Nandi, M.; Rhubright, D.; Sen, A. *Inorg. Chem.* **1990**, *29*, 3066. (b) Stecher, H.; Sen, A.; Rheingold, A. L. *Inorg. Chem.* **1989**, *28*, 3280.

(23) Ohtsuka, R.; Morioka, Y.; Kobayashi, J. *Bull. Chem. Soc. Jpn.* **1989**, *62*, 3195.

(24) Terry, K. W.; Lugmair, C. L.; Tilley, T. D., manuscript in preparation.

Scheme 1

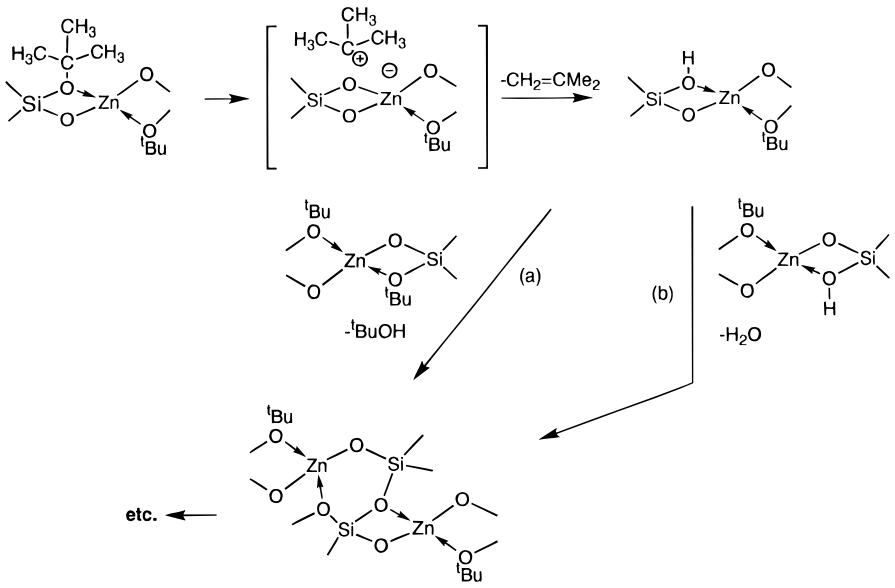

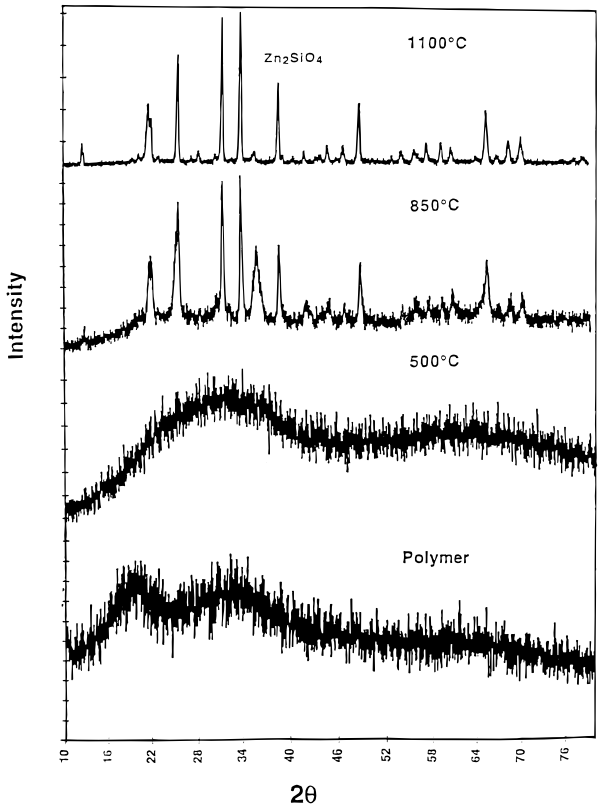

Figure 7. X-ray powder diffraction (XRD) spectra of polymer **D** and ceramic materials derived therefrom by heating to 500, 850, and 1100 °C.

temperature was increased (Figure 7). The preceramic polymer itself shows some degree of order, as evidenced by the broad diffraction peak centered at $2\theta = 19°$. This order disappears after the polymer is heated at 500 °C for 2 h and converted to an amorphous material. After the sample was heated at 850 °C for 2 h, partial crystallization to Zn_2SiO_4 was observed, consistent with observation of an exotherm in the DTA curve for **D**, at about 800 °C (Figure 6). Broad peaks at $2\theta = 25$ and 36° may arise from β-Zn_2SiO_4, which transforms to willemite above ca. 900 °C.[4d,e] Similar crystallization temperatures for zinc orthosilicate have been reported for sol-gel derived material.[4b] Samples taken to temperatures above 1100 °C exhibited only diffraction peaks for Zn_2SiO_4.

The morphology of the ceramic materials prepared at different temperatures was examined by scanning electron microscopy (SEM). Samples prepared at temperatures below 1100 °C exhibited morphologies similar to that shown in Figure 8a, with no apparent pores or channels that might have resulted from gas evolution during the ceramic conversion process. Materials heated at 1350 °C appeared to have melted (Figure 8b); however, it should be noted that the melting points for cristobalite and α-Zn_2SiO_4 are 1713 and 1512 °C, respectively. A typical TEM micrograph for material annealed at 1100 °C (Figure 4b) reveals a glassy morphology that is distinct from that of material obtained from a molecular precursor (Figure 4a), which gave particles of fairly uniform size.

Although research on synthetic routes to phosphors based on zinc orthosilicate has largely focused on the production of ceramic powders, the formation of metal-ion doped zinc orthosilicate coatings on ceramic substrates have recently been employed as thin-film electroluminescent devices.[2] The high solubility of $[ZnOSi(O^tBu)_2O]_n$ in nonpolar organic solvents suggested the use of polymer-processing routes to zinc silicate thin films. We have been able to cast high-quality thin films onto glass and quartz substrates by either spreading the polymer solution onto the substrate or by dip-coating into a 2.3% (w/w) solution of polymer **D** in 1,2-dimethoxyethane. Pyrolysis of the polymer films under an argon atmosphere (2 °C/min, 500 °C, 1 h) gave clear, smooth ceramic films. The SEM micrograph of a $Zn_2SiO_4 \cdot SiO_2$ coating on a glass slide (Figure 9) shows smooth, complete coverage of the substrate at a magnification of 15 000×. Spin-coating methods were generally more successful in producing crack-free, smooth films. The thicknesses of the films, estimated from the film edges, fell between 5−20 μm.

Synthesis of Manganese-Doped $Zn_2SiO_4 \cdot SiO_2$ Materials. Introduction of manganese into zinc orthosilicate was achieved via ceramic conversions from $[ZnOSi(O^tBu)_2O]_n$/$[Mn(CH_2SiMe_3)_2]_m$ polymer blends containing ca. 1−15% $Mn(CH_2SiMe_3)_2$ (by weight). In a typical procedure, the polymer mixtures were dissolved in diethyl ether solution and then evaporated to dryness. Pyrolysis of the resulting mixture under an argon atmosphere at temperatures above 1000 °C produced $Zn_2SiO_4 \cdot SiO_2$:Mn composites. The final manganese and zinc

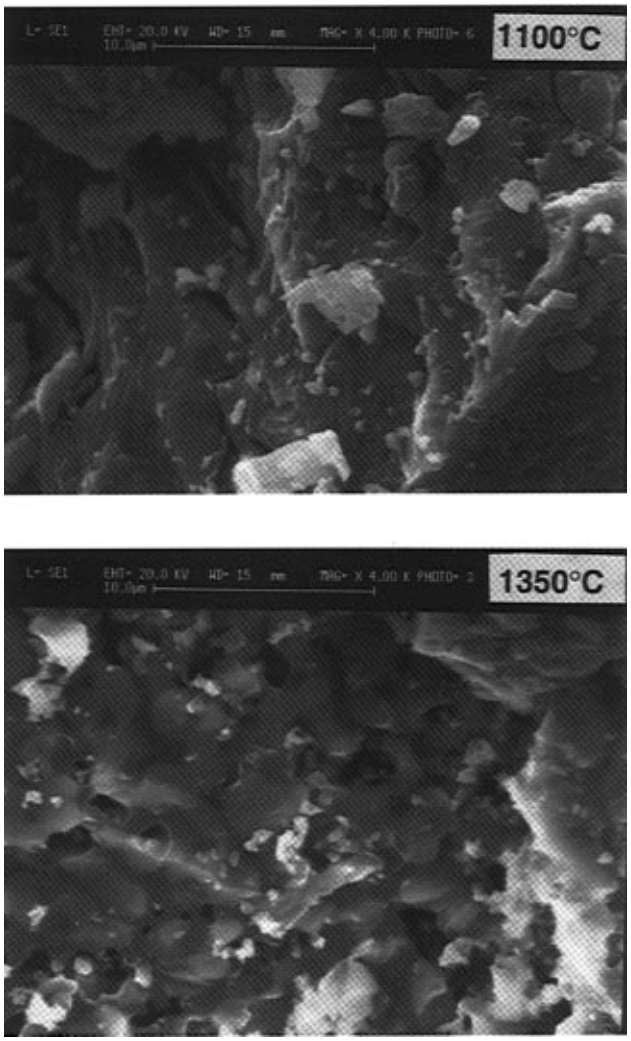

Figure 8. Scanning electron micrographs of ceramics derived from polymer **D** heated to (a) 1100 °C and (b) 1350 °C.

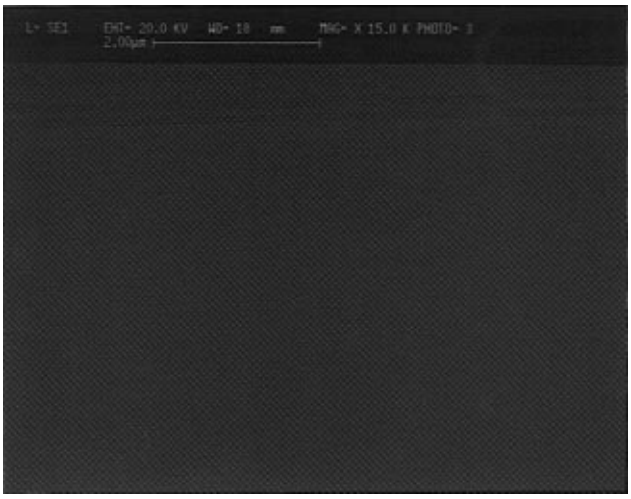

Figure 9. Scanning electron micrograph (15,000x) of a ceramic film obtained by casting polymer **D** onto a glass slide, and then heating at 500 °C for 1 h.

contents for the resulting materials were determined by inductively coupled plasma (ICP) atomic absorption analysis. The thermal decomposition behavior for these samples, examined by TGA, was very similar to that observed for the undoped polymer. As determined by ^{1}H and ^{13}C NMR spectroscopy, tetramethylsilane was the only volatile decomposition product that could be attributed to the manganese precursor compound.

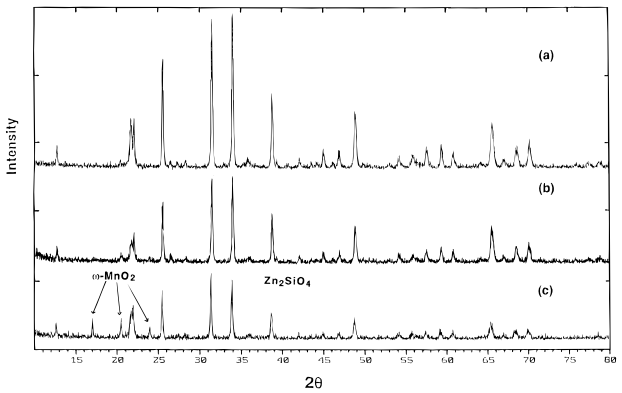

Figure 10. XRD spectra of $Zn_2SiO_4{\cdot}SiO_2$ doped with manganese ions: (a) 2.3 % Mn, (b) 3.2 % Mn, (c) 5.2 % Mn.

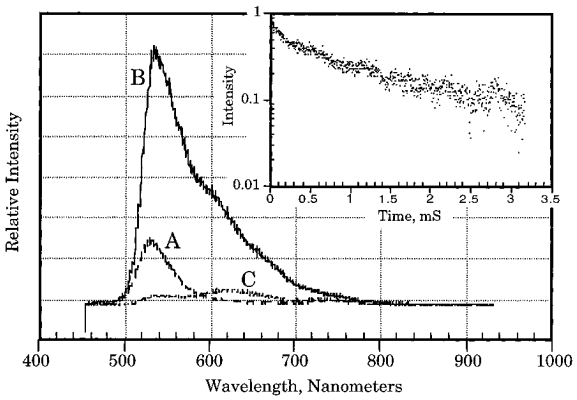

Figure 11. Fluorescence spectra of manganese-doped ceramics (1100 °C) derived from **D**. (a) 0.4 wt % Mn (b) 2.3 wt % Mn (c) 5.2 wt % Mn. Inset shows time-resolved fluorescence decay spectrum (337 nm excitation, observed at 535 nm, sample containing 2.1 wt % Mn).

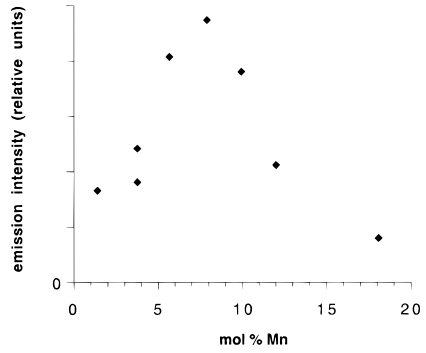

Figure 12. Plot of relative emission intensity (at 535 nm) vs manganese doping level for Mn-doped $Zn_2SiO_4{\cdot}SiO_2$ samples.

As shown by XRD patterns for the manganese-doped samples (Figure 10), the crystalline phases present after heating to 1000 °C were dependent on the amount of manganese dopant. For ceramic materials containing less than ca. 3 wt % Mn, zinc orthosilicate was observed as the only crystalline phase. However for higher manganese concentrations, a second phase, identified as ω-MnO_2 (Figure 10c), appeared. This suggests a limitation for the solubility of manganese in $Zn_2SiO_4{\cdot}SiO_2$.

Fluorescence Studies on the Zn_2SiO_4:SiO_2:Mn Materials. As shown in Figure 11, the $Zn_2SiO_4{\cdot}SiO_2$:Mn materials prepared by the above method exhibit two photoluminescence emission bands centered at 535 and 605 nm. The intensity of the green emission at 535 nm initially increases with increasing manganese concentration (Figure 12). A loss of photoluminescence quantum efficiency, attributed to concentration quenching,[1d] occurs when the Mn concentration in $Zn_2SiO_4{\cdot}SiO_2$ exceeds ca. 9 mol %. The manganese concentrations represented in

Figure 12 were calculated from the experimentally determined Mn/Zn ratios.

Photoluminescence decay measurements (Figure 12 inset) show nonsingle exponential decays. The long time component corresponds to a lifetime of approximately 5 ms, which is typical of the Zn_2SiO_4:Mn phosphor.[1] The green band at 535 nm is assigned to Mn emission from the Zn_2SiO_4:Mn phosphor, while the origin of the red emission at 605 nm is unclear. The red emission is observed in all samples studied, either as a distinct peak or as a shoulder on the green 535 nm band. There is no strong correlation between the intensities of the two emission bands from sample to sample. The red band may possibly arise from Mn in a different coordination environment, Mn in the SiO_2 phase, or from a defect such as interstitial oxygen, as has been characterized for ZnO-based phosphors.[25]

In preliminary experiments, we have also produced manganese-doped $Zn_2SiO_4 \cdot SiO_2$ thin films on quartz plates, using the methodology described above. These films display luminescent properties similar to those for the powders just described.

Conclusions

We have demonstrated that oxygen-rich molecular and polymeric alkoxy(siloxy) zinc derivatives are excellent precursors to Zn_2SiO_4, in that the ceramic conversions occur at low temperatures and give close to the theoretical yield of the zinc silicate. The conversion to solid state networks occurs without the incorporation of carbon, which is generally a problematic feature associated with organometal- and polymeric precursor routes to ceramic materials.[26] These clean conversions are perhaps facilitated by the presence of "preformed" ZnO_4 and SiO_4 tetrahedral building blocks in the precursors. In particular, the $[ZnOSi(O^tBu)_2O]_n$ "single source" preceramic polymer gives the theoretical yield for $Zn_2SiO_4 \cdot SiO_2$ and provides good routes to high-quality thin films. This behavior is in marked contrast to that for $[ZnOSiPh_2O]_n$, which decomposes to hexaphenyltrisiloxane-1,5-diol and ZnO.[7b] Previously, attempts have been made to develop sol-gel methods for producing Zn_2SiO_4, based on the cohydrolysis of zinc and silicon alkoxides, with the goal of producing more homogeneous materials via the formation of Zn−O−Si linkages in solution. However, such methods also tend to result in production of ZnO as a side product.[4a,d]

It appears that the precursors described here provide considerable (perhaps atomic-level) control over the homogeneity of the resulting silicate, since no zinc oxide was detected in any of the ceramic conversion processes examined (by XRD). In addition, we observe that this approach allows for relatively fine control over the emission intensity of the resulting Zn_2SiO_4:Mn phosphors. Similar observations have been made for sol-gel derived phosphors, which exhibit a maximum in the photoluminescence intensity at a Mn doping level of ca. 2 mol %.[4a] From the data presented in Figure 12, it appears that Zn_2SiO_4:Mn material produced by the polymer route described here *may* be doped to higher levels (ca. 8−9 mol % in $Zn_2SiO_4 \cdot SiO_2$) before concentration quenching occurs. If this is true, then an obvious implication is that perhaps our use of partially "prefabricated" precursors has achieved a more homogeneous distribution of manganese ions in the zinc orthosilicate lattice. However, this conclusion is tentative since the distribution of manganese ions between the Zn_2SiO_4 and SiO_2 phases is not known. Future studies are intended to address this issue, via development of precursors which convert solely to Zn_2SiO_4. Given the inherent flexibility of the approach described here, it may prove possible to accomplish this simply by using two-component precursor mixtures such as $[ZnOSi(O^tBu)_2O]_n$/$ZnMe_2$ or $[ZnOSi(O^tBu)_2O]_n$/$Zn(OR)_2$.

Acknowledgment. This work was supported by the Director, Office of Energy Research, Office of Basic Energy Sciences, Chemical Sciences Division, of the U.S. Department of Energy under Contract No. DE-AC03-76SF00098. We also thank Dr. Fred Hollander of the departmental X-ray facility (CHEXRAY) for determination of the crystal structure. M.J.S. thanks the A. P. Sloan Foundation and the Camille and Henry Dreyfus foundation for support. We thank a reviewer for helpful comments.

Supporting Information Available: Notes on solution of the structure, additional views of the molecule, and tables of crystal, data collection, and refinement parameters, bond distances and angles, and anisotropic displacement parameters (19 pages). This material is contained in many libraries on microfiche, immediately follows this article in the microfilm version of the journal, can be ordered from ACS, and can be downloaded from the Internet; see any current masthead page for ordering information and Internet access instructions.

JA9537639

(25) Liu, M.; Kitai, A. H.; Mascher, P. *J. Luminescence* **1992**, *54*, 35−42.

(26) See for example: (a) Cowley, A. H.; Jones, R. A. *Angew. Chem. Int. Ed. Engl.* **1989**, *28*, 1208. (b) Seyferth, D.; Wiseman, G. H.; Schwark, J. M.; Yu, Y.-F.; Poutasse, C. A. In *Inorganic and Organometallic Polymers*; Zeldin, M., Wynne, K. J., Allcock, H. R., Eds.; ACS Symposium Series 360; American Chemical Society: Washington, DC, 1988; p 143.